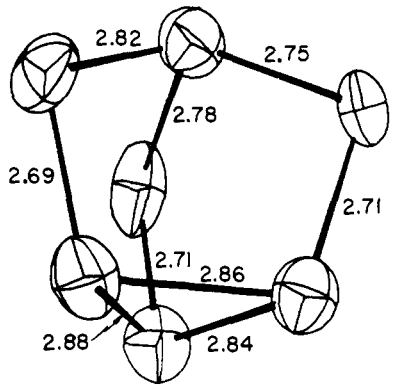

Figure 1. Configuration of the ion Sb_7^{3-} in the salt $[Na(crypt)^+]_3Sb_7^{3-}$

dry en produces a deep brown solution in 10-15 min. Evaporation of the solvent yields brown needles and chunks that have been shown to be $[Na(crypt)^+]_3Sb_7^{3-}$ (see below). No other phase appears to be formed from Na-Sb alloys save for small amounts of the blue "sodium crypt electronide"[10] obtained from samples with the higher sodium activities.

The compositions $NaSn_{2.25}$ and $NaSn_{1.32}$ both dissolve in en alone[8] and redeposit alloy on thorough solvent removal, but crypt complexation allows the isolation of intensely colored orange-red needles and rods in pure form. The coloration is similar to that reported by others for Sn_9 derivatives.[3,4,8] The compound is somewhat unstable to X-rays but usable data can be secured when the crystal is cooled. Use of $Na_{1.7}Sn$ yields a more reduced yellow-brown polytin phase, a coloration also noted in liquid ammonia solutions.[11] The compositions $NaPb_{2.25}$, $NaPb_{1.75}$, and $NaPb_{1.3}$ all dissolve relatively rapidly in en only in the presence of crypt, but these redeposit brown mud and rods which are only polycrystalline composites of the alloy phase $MPb_{2.2}$. However, slow refluxing of a solution of $NaPb_{1.3}$ and crypt in en at ~90° gives a low yield of ruby red crystals which are close to $[Na(crypt)^+]_4Pb_9^{4-}$ in composition but which do not have the green color associated with Pb_9^{4-} in liquid ammonia.[4,11] The sodium-bismuth-crypt reactions appear to be the most complex and, among those systems considered, the least productive of good crystals. Samples of NaBi or NaBi + Bi react with crypt in en to produce an immediate blue-green color, and this eventually deepens to a dichroic green-ruby red solution. No coloration is observed with en alone. The crypt solution deposits a microcrystalline green to rose colored polybismuth salt on evaporization of solvent.

X-Ray data have been obtained from a single crystal of the polyantimony derivative described above with a four-circle automatic diffractometer using Mo $K\alpha$ radiation. The monoclinic cell dimensions are a = 23.292 (7) Å, b = 13.791 (6) Å, c = 25.355 (6) Å, β = 108.56 (2)°, and observed extinctions uniquely fixed the space group as $P2_1/n$. Utilizing 4662 unique reflections with $I_{obsd} > 3\sigma_I$ the correct location of the seven antimony atoms in general positions was deduced by direct methods.[12] Successive refinement followed by electron density synthesis located three sodium atoms and, after some care, the three independent crypt molecules surrounding the sodium atoms. Full-matrix least-squares refinement of all 88 independent (nonhydrogen) atoms with anisotropic thermal parameters for the ten heavy atoms and isotropic parameters for those in the crypt ligands yielded a conventional R of 0.111 and a difference Fourier map with ripples <5 e/Å^3 near the antimony atoms and ≤±1 e/Å^3 elsewhere.

The most remarkable feature of the structure is the Sb_7^{3-} ion, Figure 1, in which the atoms occur in an end-capped trigonal prism of approximately C_{3v} symmetry with the capped face opened up to substantially nonbonding distances (4.19-4.34 Å). The Sb_7^{3-} ion is the first characterized polyatomic anion of a metallic element although it is quite similar in configuration and presumably bonding to that briefly described for P_7^{3-} (in the ionic limit) in the phase Sr_3P_{14} prepared at high temperatures.[13] The three sodium-crypt cations exhibit configurations and average distances which are quite comparable to those found in $Na(crypt)^+I^-$.[14]

In general a fertile synthetic field appears indicated, and several derivatives are presently under structural investigation.

References and Notes

(1) 4,7,13,16,21,24-hexaoxa-1,10-diazobicyclo[8.8.8]hexacosane, $N(C_2H_4OC_2H_4OC_2H_4)_3N$.
(2) B. Dietrich, J. M. Lehn, and J. P. Sauvage, *Tetrahedron Lett.*, **34**, 2885 (1969).
(3) E. Zintl, J. Goubeau, and W. Dullenkopf, *Z. Phys. Chem., Abt. A*, **154**, 1 (1931).
(4) E. Zintl and A. Harder, *Z. Phys. Chem., Abt. A*, **154**, 47 (1931).
(5) E. Zintl and W. Dullenkopf, *Z. Phys. Chem., Abt. B*, **16**, 183 (1932).
(6) H. Schafer, B.Eisenmann, and W. Müller, *Angew. Chem., Int. Ed. Engl.*, **12**, 694 (1973).
(7) M. Okada, R. A. Guidotti, and J. D. Corbett, *Inorg. Chem.*, **7**, 2118 (1968).
(8) D. Kummer and L. Diehl, *Angew. Chem., Int. Ed. Engl.*, **9**, 895 (1970).
(9) M. T. Lok, F. J. Tehan, and J. L. Dye, *J. Phys. Chem.*, **72**, 2975 (1972).
(10) F. J. Tehan, B. L. Barnett, and J. L. Dye, *J. Am. Chem. Soc.*, **96**, 7203 (1974).
(11) C. A. Kraus and H. F. Kurtz, *J. Am. Chem. Soc.*, **47**, 43 (1925).
(12) P. Main, M. M. Woolfson, and F. Germain, "MULTAN, A Computer Program for the Automatic Solution of Crystal Structures", University of York Printing Unit, York, U.K., 1971.
(13) W. Dahlmann and H. G. v. Schnering, *Naturwissenschaften*, **59**, 420 (1972).
(14) D. Moras, B. Metz, and R. Weiss, *Acta Crystallogr., Sect. B*, **29**, 396 (1973).

John D. Corbett,* Douglas G. Adolphson, Don J. Merryman
Paul A. Edwards, Frank J. Armatis
Ames Laboratory-ERDA and Department of Chemistry
Iowa State University
Ames, Iowa 50010
Received July 17, 1975

Molecular Beam Chemistry. Reactions Exchanging van der Waals Bonds among Three or More Halogen Molecules

Sir:

Under the single-collision conditions provided in crossed-beam experiments, $Br_2 + Cl_2$ at collision energies up to ~25 kcal/mol yields no product attributable to bimolecular reaction.[1] However, even at thermal collision energies of only ~3 kcal/mol evidence was found[2] for a facile termolecular reaction,

$$Br_2 + Cl_2 \cdots Cl_2 \rightarrow 2BrCl + Cl_2 \qquad (R1)$$

The dimeric chlorine reactant, $Cl_2 \cdots Cl_2$, is held together by a weak van der Waals bond[3] with dissociation energy ~1-2 kcal/mol and bond length ~4.3 Å. Here we report further experiments which confirm (R1) and give evidence for two other facile reaction paths,

$$Br_2 + Cl_2 \cdots Cl_2 \rightarrow BrCl \cdots Cl_2 + BrCl \qquad (R2)$$

$$Br_2 + Cl_2 \cdots Cl_2 \rightarrow Br_2 \cdots Cl_2 + Cl_2 \qquad (R3)$$

The (R2) path is a corollary of the reaction sequence suggested for the (R1) process.[2] Six-center bond exchange is assumed to occur in a cylic transition state which disso-

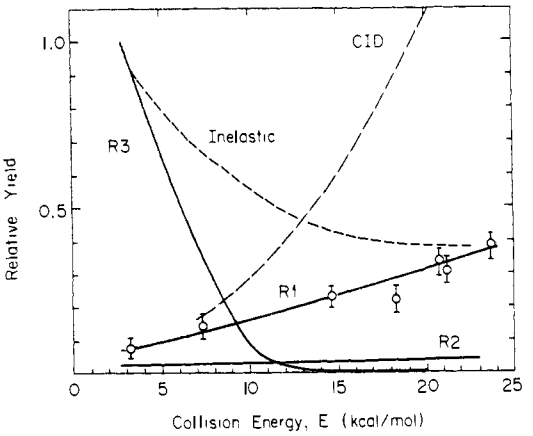

Figure 1. Variation of yields with initial relative translational energy for five $Br_2 + (Cl_2)_2$ collision processes: reactions producing (1) BrCl, (2) $BrCl_3$, and (3) Br_2Cl_2; inelastic scattering producing vibrationally excited $(Cl_2)_2$; and collision induced dissociation (CID) producing $Cl_2 + Cl_2$. Experimental points are included for reaction (1) to illustrate quality of the data. These results pertain to a laboratory scattering angle of 70° (cf. Figure 2) but similar results were found at 80°. Relative normalization of yields was derived from observed intensity ratios but uncertain by at least a factor of 2 for any pair of processes due to uncertainty in mass spectrometric detection efficiency and other factors. Absolute cross section for reaction 3 is estimated to be of the order 5-50 Å^2.

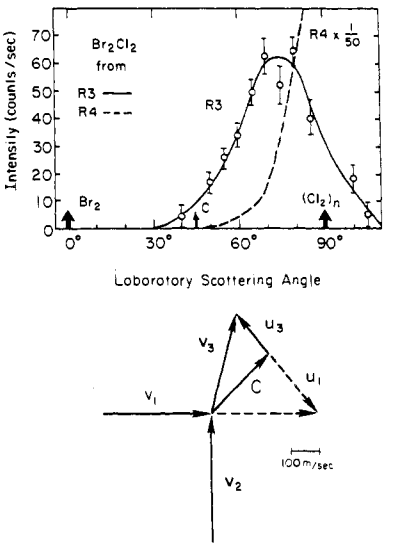

Figure 2. Angular distribution of Br_2Cl_2 from reaction of Br_2 with $(Cl_2)_2$ (R3, solid curve from data taken at 250 Torr chlorine source pressure), and from reaction with higher chlorine polymers (R4, dashed curve from data taken at 800 Torr source pressure). Collision energy was 3.4 kcal/mol. Vector diagram shows for R3 reaction the most probable reactant beam velocities (bromine denoted by v_1, chlorine dimer by v_2) and most probable product Br_2Cl_2 velocity (denoted by v_3), as determined from angular distribution and time-of-flight data. Also shown are directions of corresponding centroid vector (denoted **C**) and velocity vectors relative to centroid ($\mathbf{u} = \mathbf{v} - \mathbf{C}$) for Br_2 and for Br_2Cl_2.

ciates via a chain structure, $BrCl\cdots Cl_2\cdots ClBr$. The observed product angle-velocity distributions for (R1) indicate one of the $BrCl\cdots Cl_2$ van der Waals bonds breaks before the other. Thus (R2) occurs when the second of these weak bonds does not break. Comparison of the angle-velocity distributions for (R2) and (R1) is quantitatively consistent with this interpretation, as shown elsewhere.[4] Figure 1 includes a comparison of the reaction yields and the dependence on collision energy, which likewise proves consistent, in that (R1) exceeds (R2) and the ratio increases with energy. This paper deals chiefly with (R3) and related processes involving higher chlorine polymers; these offer examples of reactions involving exchange of van der Waals bonds among molecules.

As in our previous studies,[1,2] the chlorine beam was obtained from a supersonic nozzle source. The fraction of dimers $(Cl_2)_2$ and higher polymers in the beam can be varied over a wide range by adjusting the source parameters. Except as noted below, the conditions used in these experiments were: source pressure ~200-250 Torr, temperature ~290 K, nozzle diameter ≳0.06 mm, and nozzle-to-skimmer distance ~5 mm. For these conditions the $(Cl_2)_2$ fraction is a few per cent but trimers and higher polymers are almost undetectable.[4] The Br_2 beam was also obtained from a supersonic nozzle, operated at ~70 Torr and 425 K to prevent dimer formation. The collision energy was scanned up to ~25 kcal/mol by "seeding" the Br_2 at ~10 Torr in an excess of helium, up to ~350 Torr. The reactant beams were monitored and the products detected by a mass spectrometer equipped with a time-of-flight velocity analyzer.[5] The much improved source and detector conditions revealed that the observed BrCl, $BrCl_3$, and Br_2Cl_2 signals all correlate with the $(Cl_2)_2$ concentration, whereas the marked differences found in the energy dependence of Figure 1 and the product angle-velocity distributions show these signals come from three distinct reaction modes.

Since (R3) does not disrupt chemical bonds and only requires Br_2 to interact with the nearer Cl_2 molecule of the dimer, this reaction path is accessible for many noncylic collisional orientations for which (R2) and (R1) cannot occur. The preponderance of such noncylic configurations probably accounts for the predominance of (R3) seen in Figure 1 at low collision energies, but (R3) declines rapidly at higher collision energies and becomes much less probable than collision-induced dissociation to form $Br_2 + Cl_2 + Cl_2$. Figure 2 shows the reactively scattered Br_2Cl_2 from (R3) recoils backwards with respect to the incident Br_2 molecules. The Br_2Cl_2 velocity distribution indicates the reaction has a small but perceptible energy release into product translation.[6] This is of the order of a few tenths of a kilocalorie per mole and thus comparable to the expected difference in the $Br_2\cdots Cl_2$ and $Cl_2\cdots Cl_2$ van der Waals bond strengths. Both the backward recoil and the energy release into translation observed for (R3) are analogous to the "rebound" behavior found for a large class of atom + diatomic molecule reactions.[7]

Reactions corresponding to (R1), (R2), and (R3) have also been studied in the same way for the HI + $(Cl_2)_2$ system. Again, rebound behavior was found for (R3) and the $HICl_2$ velocity indicates a reaction exoergicity of a few tenths of a kilocalorie per mole.

The scattering of higher chlorine polymers $(Cl_2)_n$ was examined using source pressures up to ~800 Torr. Comparison of the product angle-velocity distributions for low and high chlorine source pressures shows very little change for BrCl and $BrCl_3$. However, as shown in Figure 2, the Br_2Cl_2 angular distribution undergoes a drastic change in shape. This indicates a large contribution from reactions involving higher polymers, such as

$$Br_2 + (Cl_2)_n \rightarrow Br_2Cl_2 + (Cl_2)_{n-1} \qquad (R4)$$

In the high pressure regime, large yields of $Br_2(Cl_2)_m$ polymers with $m = 2, 3, \ldots$ also appear.[8] These might come from $Br_2 + (Cl_2)_n$ reactions with a range of $n \geq m$, since fragmentation in the mass spectrometer may contribute substantially to the $Br_2(Cl_2)_m$ signals. A correlation between n and m nevertheless was found on reducing the chlorine source pressure. As illustrated in Figure 3, the $Br_2(Cl_2)_m$ signals for $m = 3$-1 become undetectably small

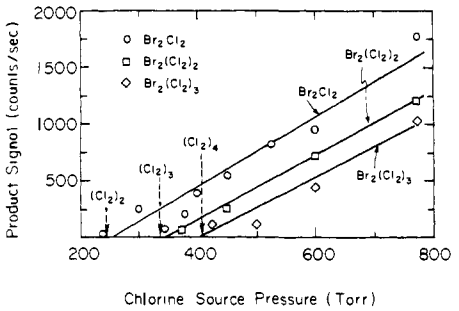

Figure 3. Variation with chlorine source pressure of scattered $Br_2(Cl_2)_m$ product molecules with m = 1-3 from reaction of Br_2 with chlorine polymers. Data pertain to a laboratory scattering angle of 70° (cf. Figure 2) and collision energy of 3.4 kcal/mol. Arrows indicate nominal "pressure thresholds" below which $(Cl_2)_n$ signals become very small.

below certain source pressures and the $(Cl_2)_n$ signals for n = 4-2, respectively, disappear below these same "pressure thresholds". This indicates that at least the regions between successive thresholds are governed by van der Waals exchange reactions of the form

$$Br_2 + (Cl_2)_n \rightarrow Br_2(Cl_2)_{n-1} + Cl_2 \qquad (R5)$$

As in the (R3) case, where n = 2, these reactions with n = 3 or 4 appear to be rebound processes. Results corresponding to (R4) and (R5) were also found for reactions of HI and CH_3Br with chlorine polymers.[9]

Recently, $Br_2 + (Cl_2)_n$ reactions in the high polymer regime have been studied in crossed-beams by Behrens et al.[10] Comparable aspects agree with our results. However, most of their work is complementary; it deals with larger polymers and scattering within 10° of the chlorine beam, which we did not study for high polymers. Behrens et al. find evidence for "condensation" to form $Br_2(Cl_2)_n$ adducts which for $n \gtrsim 10$ persist long enough ($\gtrsim 10^{-5}$ sec) to travel to the detector. Other polymer systems with large n also appear to form such adducts under single-collision conditions.[10-12] More complex polymer reactions, including proton transfer and solvation processes, have also been observed in beam experiments.[13] There is now much scope for reactive scattering studies of the weak but ubiquitous van der Waals bonding.

Acknowledgments. We wish to thank R. R. Herm for correspondence about his related work and to acknowledge gratefully support of this study by the National Science Foundation.

References and Notes

(1) D. A. Dixon, D. L. King, and D. R. Herschbach, *Faraday Discuss. Chem. Soc.*, **55**, 360 (1973).
(2) D. L. King, D. A. Dixon, and D. R. Herschbach, *J. Am. Chem. Soc.*, **96**, 3328 (1974).
(3) S. J. Harris, S. E. Novick, J. S. Winn, and W. Klemperer, *J. Chem. Phys.*, **61**, 3866 (1974).
(4) D. A. Dixon, Ph.D. Thesis, Harvard University, 1975. D. A. Dixon, D. L. King, and D. R. Herschbach, *J. Am. Chem. Soc.*, to be submitted for publication.
(5) Since the work of ref 2, the electron bombardment ionizer and parts of the ion counting system have been rebuilt, with considerable improvement in detection sensitivity. This allowed use of a smaller chlorine nozzle and lower source pressure as well as higher mass resolution (~1%). Fragmentation in the electron bombardment region appears not to introduce significant ambiguity when higher chlorine polymers are absent. Some of the $BrCl^+$ signal could come from fragmentation of $BrCl_3^+$, since (R1) and (R2) are parallel paths with somewhat similar properties, but very little of the $BrCl^+$ can be attributed to fragmentation of $Br_2Cl_2^+$, in view of the drastic difference in the energy dependence and angular distribution for (R1) and (R3).
(6) Only a rough estimate can be obtained for the difference ΔE_T between the product and reactant relative translational energy because it is smaller than the spread in collision energy. Also, momentum conservation imposes constraints because the detected product Br_2Cl_2 is much heavier than its partner Cl_2. The difference ΔD_0 in the $Br_2\cdots Cl_2$ and $Cl_2\cdots Cl_2$ van der Waals bond strengths is related to the energy disposal in translation, vibration, and rotation by $\Delta D_0 = \Delta E_T + \Delta E_{V+R}$. The use of supersonic beams makes $E_{V+R} \sim 0$ for the reactants, so $\Delta E_{V+R} \gtrsim 0$ and $\Delta D_0 \gtrsim \Delta E_T$. The lower bounds probably apply in view of the weak bonds involved. Analysis of the data gives nominal most probable values of ΔE_T = 0.4 and 0.5 kcal/mol for the Br_2 and HI versions of (R3), respectively.
(7) D. R. Herschbach, *Faraday Discuss. Chem. Soc.*, **55**, 233 (1973).
(8) Molecules of the form $BrCl(Cl_2)_m$ with m = 2 or 3 were not observed.
(9) The (R5) reaction to form $Br_2(Cl_2)_2$ or $HI(Cl_2)_2$ is of particular interest. (R1) allows cyclic configurations of these n = 3 species to undergo facile six-center reaction (exoergic by 20 kcal/mol for the HI case). The cyclic configurations might be stable if formed in a "van der Waals well", but excitation of only a few kilocalories per mole would permit the six-center reaction. Stereochemical arguments as well as the observed resemblance of the Br_2, HI, and CH_3Br reactions suggest (R5) probably forms noncyclic polymers.
(10) R. Behrens, A. Freedman, R. R. Herm, and T. P. Parr (private communication, Iowa State University).
(11) A. G. Urena, R. B. Bernstein, and G. R. Phillips, *J. Chem. Phys.*, **62**, 1818 (1975).
(12) J. T. Cheung, D. A. Dixon, and D. R. Herschbach, *J. Am. Chem. Soc.*, to be submitted for publication.
(13) For example, ref 4 and 12 report HI + $(NH_3)_n$ in crossed-beams yields $NH_4^+I^-(NH_3)_m$; molecules with n up to 21 and m = 2-13 were observed.

D. A. Dixon, D. R. Herschbach*
Department of Chemistry, Harvard University
Cambridge, Massachusetts 02138
Received July 10, 1975

The Absolute Configuration of Vincoside

Sir:

The intricate pathway by which the structurally diverse indole and dihydroindole alkaloids are biosynthesized in several Apocynaceous plants has been elucidated by decisive research in several laboratories.[1] The keystone of this pathway is vincoside (**1a**), which results in vivo and in vitro along with isovincoside (strictosidine), **1b**, from the condensation of tryptamine with secologanin.[2] Originally,[2] **1a** was depicted with a C-3 (*S*) α-hydrogen, which was cis to the C-15 and C-20 hydrogens whose absolute configurations were known by correlation with loganin.[3] Such an assignment also seemed sensible since the Corynanthé alkaloids into which **1a** was shown to be efficiently incorporated[2] are *S* at C-3.[4] Smith[5] and Brown[6] and coworkers subsequently reported chemically and spectroscopically derived results that were discordant with Battersby's assignment, favoring instead a C-3 (*R*) β hydrogen for **1a**. Simultaneously, Battersby et al. revised the absolute C-3 stereochemistry of **1a** to *R* by implication from its comparison to *O,O*-dimethylipecoside, its tetrahydroisoquinoline analog, using X-ray analysis.[7] In view of the special significance of **1a** and **1b**[8] in the developing picture of indole alkaloid biosynthesis, we felt that an X-ray analysis of **1a** was necessary to absolutely secure its stereochemistry. Additionally, we have correlated **1c** to its lactam[2] (**2a**),[10] to its pentaacetyl 7-oxo-pyrrolo[3,4-*b*]quinoline derivative[9] (**3a**)[10] to provide readily accessible, crystalline standards of C-3 stereochemistry, and to the now

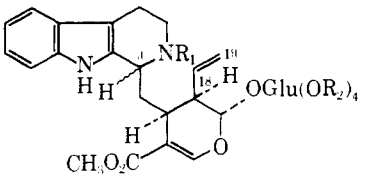

1a, C-3 *R* (βH), $R_1 = R_2 = H$
1b, C-3 *S* (αH), $R_1 = R_2 = H$
1c, C-3 *R* (βH), $R_1 = CH_2C_6H_4Br$; $R_2 = COCH_3$
1d, C-3 *R* (βH), $R_1 = R_2 = CO_2CH_2CCl_3$
1e, C-3 *S* (αH), $R_1 = R_2 = CO_2CH_2CCl_3$